
		Deliverable ID: <b>D4.1</b>	Preparation date: <b>03 April 2019</b>
 Terahertz based Ultra High Bandwidth Wireless Access Networks		Milestone: Final Proposed	
		Title:  <b>Initial characterization of devices</b>	
		Editor/Lead beneficiary (name/partner): <b>Mira Naftaly/ NPL</b>	
		Internally reviewed by (name/partner): <b>Johannes Eckhardt/ TUBS</b> <b>Diego Moro-Melgar/ ACST</b>	
		Approved by: <b>PSC</b>	
<b>Dissemination level</b>			
<b>PU</b>	Public		
<b>CO</b>	Confidential, only for members of the consortium (including Commission Services)		

Revisions				
Version	Date	Author	Organisation	Details
<b>0.1</b>	21/08/18	Mira Naftaly	NPL	Initial version
<b>0.2</b>	03/9/18	Mira Naftaly	NPL	Updated following internal review by TUBS
<b>0.3</b>	13/9/18	Mira Naftaly	NPL	Updated following internal review by ACST
<b>0.4</b>	02/10/18	Mira Naftaly	NPL	Updated following review by PSC

# Table of contents

- Table of contents ..... 2
- List of figures ..... 3
- Executive summary ..... 4
- 1 Introduction ..... 5
  - 1.1 Summary ..... 5
  - 1.2 Structure of this document ..... 5
  - 1.3 Relationships with other deliverables ..... 5
  - 1.4 Contributors ..... 5
- 2 Device characterisation ..... 6
  - 2.1 Instruments for device characterisation ..... 6
    - 2.1.1 Power measurement ..... 6
    - 2.1.2 Lamellar interferometer ..... 7
    - 2.1.3 Emitter beam profile ..... 9
  - 2.2 Results ..... 10
    - 2.2.1 Broadband frequency measurements ..... 10
    - 2.2.2 Beam profile measurements ..... 11
- 3 Conclusion/Further work ..... 12
- References ..... 13

## List of figures

Figure 1. Photograph of the SLT pyroelectric detector.....	6
Figure 2. Spectral responsivity, from Ref. 2. ....	7
Figure 3. Schematic drawing of a lamellar interferometer and a split mirror. ....	8
Figure 4. Photograph of the lamellar split mirror at NPL. ....	9
Figure 5. Schematic drawing of beam imaging by aperture scanning. ....	10
Figure 6. Frequency measurements using lamellar interferometer and Toptica source at 300 GHz: a) interferometer signal; b) calculated spectrum. ....	10
Figure 7. Beam profiles from Toptica emitter at different frequencies, measured along the horizontal and vertical axes. ....	11
Figure 8. Beam profile from Menlo emitter and a Gaussian fit (data from two axes overlap).....	11

## Executive summary

This deliverable is the initial report on device characterisation. It describes the characterisation instruments built for the project, and reports initial results of device measurements.

# **1 Introduction**

## **1.1 Summary**

This deliverable is the initial report on device characterisation. Section 1 describes the equipment that was designed and built for characterising devices, specifically a lamellar interferometer for measuring broadband frequency spectrum, and a setup for determining the beam profile of emitters. Section 2 reports results of measurements which demonstrate operation of the characterisation equipment. In order to test and validate characterisation equipment, measurements were carried out on two commercial emitters, consequent to the delay in the delivery of devices by the project partners. The delay has been due to the lack of availability of the clean room at UCL and the low yields from dicing and thinning the devices at UGLA. These issues have now been resolved, and the route has been agreed by the project partners for the delivery of devices to NPL within the next 3 months. Work on refining the operation of the instruments will proceed as planned.

## **1.2 Structure of this document**

This document contains two parts. The first part describes the characterisation instruments that were designed and built for the purpose; while the second part reports results of device measurements that demonstrates and validate operation of this instrumentation. The final section outlines future work.

## **1.3 Relationships with other deliverables**

This deliverable is related to WP3 and WP5.

## **1.4 Contributors**

The following partners have contributed to this deliverable: NPL.

## 2 Device characterisation

Device characterisation work in this deliverable focused on two aspects: broadband frequency measurements, and emitter beam profile measurements.

Work took place in two stages: setting up the characterisation instruments; and carrying out measurements on devices. Since no TERAPOD devices have yet been delivered by the project partners, characterisation work was performed on available commercial devices.

### 2.1 Instruments for device characterisation

#### 2.1.1 Power measurement

Pyroelectric detectors are the most widely used THz detectors / power meters. This is because they operate at room temperature and are extremely broadband ( $\sim 0.05\text{-}10$  THz) and have frequency-independent responsivity. The bandwidth and frequency insensitivity are due to the specialized absorptive coating (as is the case for all similarly broadband detectors, see below). The sensing element is pyroelectric material: absorbed radiation causes its temperature to rise, producing a change in its permanent electric dipole moment, which can be monitored in either current or voltage mode. Because signal is generated by temperature changes, only variations in absorbed radiation produce detectable signal, and therefore only on-off (or varying) power signal can be detected. The pyroelectric element is often coated with absorber in order to increase responsivity and the frequency range. For pyroelectric THz power meters, the on-off switching frequency must be very slow, typically 10-100 Hz. Pyroelectric detectors are robust, compact, inexpensive and convenient to use. They can also be traceably calibrated. In recent years PTB (Physikalisch-Technische Bundesanstalt) together with SLT (Sensor und Lasertechnik) have developed a calibrated THz power meter with spectrally flat response from 0.3 THz to 10 THz and sensitivity down to a few  $\mu\text{W}$  [1,2], shown in Figures 1 and 2. The pyroelectric detector used by NPL was an SLT unit calibrated by PTB, with the responsivity of  $1.43 \times 10^4$  V/W.

Other THz power detectors with similar functionality to pyroelectric are: the Golay cell, thermopile, and calorimeter. The Golay cell is a type of acousto-optic sensor. Radiation is absorbed by a thin metal layer, which heats the gas in a cell and raises its pressure; the cell has a flexible mirror wall whose deformation is optically detected as signal. The Golay cell has the highest sensitivity of all room-temperature THz detectors, but has two severe disadvantages. Its dynamic range is limited due to low damage threshold, typically  $10 \mu\text{W}$  (crucially, a Golay cell can be damaged by exposure even when it is switched off). Even more importantly, the responsivity of a Golay cell changes with time and exposure, and is non-linear with power, so a Golay cell cannot be employed as a calibrated power meter.

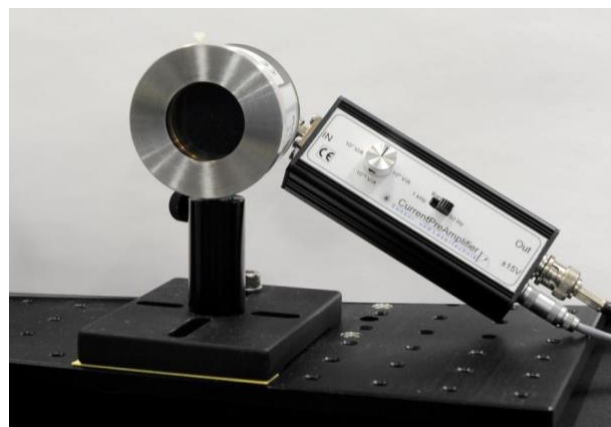
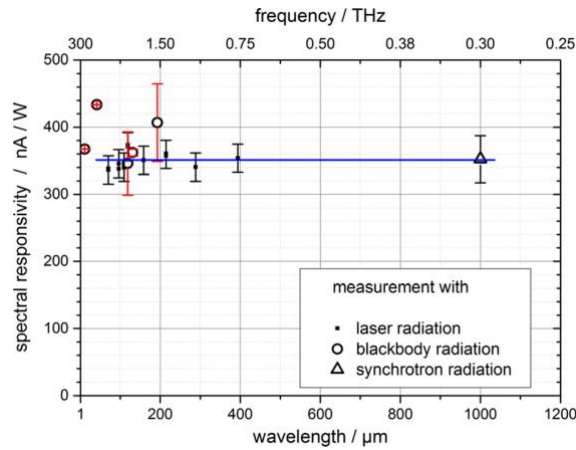


Figure 1. Photograph of the SLT pyroelectric detector.



**Figure 2. Spectral responsivity, from Ref. 2.**

A thermopile detector consists of a series array of thermocouples using the thermoelectric (Peltier) effect to convert a thermal gradient created by absorbed radiation into an electrical signal. Thermopile detectors have lower responsivity than pyroelectric, and much longer response times, making them less attractive.

A calorimeter can have sensitivity comparable to a pyroelectric detector, and can be calibrated as a power meter. Indeed, one such device, the VDI-Erickson, has been adopted as a de-facto industry standard. An isothermal calorimeter has two identical radiation inputs: radiation is coupled into one, while the other is electrically heated to equal temperature. The electrical power is then equal to the absorbed radiation power. In usage, it has two disadvantages: its response time is extremely slow (minutes for microwatt power levels); and the available instruments are designed for waveguide input, making them unsuitable for free-space measurements.

### 2.1.2 Lamellar interferometer

Heterodyne detection has long been established as the most widely-used, accurate, high-resolution, traceably calibrated technique for measuring signal frequencies and spectral profiles. It is used across the whole of the electromagnetic spectrum, from the optical down to millimeter-wave and RF. Heterodyne measurements use a local oscillator (LO) of known frequency, amplitude and phase. This is fed together with the source signal into a mixing device, which produces a signal at the difference frequency that is proportional to the amplitude of the source. The output low-frequency signal can then be easily detected and analyzed using low-frequency circuits. The principle is employed in many high-frequency instruments, including VNAs (vector network analyzers) and signal (or spectrum) analyzers. The center frequencies and linewidths of narrow-band THz emitters can thus be measured with great accuracy and resolution by heterodyne-based techniques and instruments. However, because the input to the instrument is via a waveguide, free-space devices must be coupled in using a horn antenna or a similar element. Moreover, the bandwidth of each measurement is limited by the transmission band of the waveguide. For these reasons, signal analyzers are unsuitable for characterizing the spectra of sources that produce extended frequency side-lobes, or harmonics, or have a broad spectral profile.

In such cases, a free-space broadband optical interferometer may be employed to reveal the full source spectrum. The interferogram produced by the device is a Fourier transform of the source spectrum, which therefore can be recovered by applying an FFT (fast Fourier transform) algorithm to the acquired data. Because such instruments operate in free-space, their bandwidth is not limited by waveguide transmission. In order to fully characterize a THz emitter, its spectrum must be measured using both a narrow-band heterodyne signal analyzer and a broadband free-space optical interferometer, which is the focus of NPL work.

An alternative instrument for broadband spectral measurements is the grating spectrometer, where a grating is employed to reflect the incident beam into angular dispersion. The beam spectrum can then be detected by angle-scanning. However, designing such spectrometer for quasi-optical THz beams is extremely challenging. Moreover, the grating efficiency and angular dispersion are frequency-dependent, limiting the operation bandwidth. (E.g. an optical spectrometer typically performs over an octave of wavelengths, whereas a THz spectrometer is required to cover at least 0.05-3 THz.)

A type of interferometer that is particularly suitable for broadband spectroscopy at THz frequencies is a Michelson interferometer with a lamellar mirror, shown in Figure 3, where a split mirror acts as both a beam-splitter and a moveable mirror [3]. The lamellar mirror consists of two parts, each comprising several lamellae or “fingers”, with one part being fixed and the other moveable. This design avoids using a separate beam-splitting element; has close to 100% throughput; is polarization-insensitive; and can be ultra-broadband.

Avoiding the use of a transmission beam-splitter is particularly desirable for a THz interferometer, because the maximum achievable throughput is 50%, and due to the lack of beam-splitting components fulfilling all necessary requirements. To characterize the wide variety of broadband THz beams, the splitter must be ultra-broadband, polarization-insensitive, and avoid formation of internal standing waves (since the majority of THz sources are coherent); moreover, due to low power available from most THz sources, throughput losses must be minimized. A wire-grid polarizer – the preferred choice – can offer acceptable bandwidth and the absence of standing waves, but is polarization-dependent. A semi-metallized pellicle is polarization-insensitive and has no standing waves, but is frequency-dependent. Fresnel reflectors have reduced throughput and standing waves, and are frequency-dependent. Therefore a solution requiring no beam-splitter is strongly preferred.

A lamellar interferometer can be used to determine the spectral performance of both emitters and detectors. Of particular interest as regards emitters is the possible presence of features outside the fundamental emission line, such as harmonics and side-lobes, and their dependence on the bias voltage. Since emitters employed in wireless links are supposed to be narrow-line single-frequency sources, the presence of extraneous spectral features would reveal possible malfunction or operational flaws. To characterize an emitter, a calibrated power detector is required, having a flat response over the bandwidth of interest. The pyroelectric detector described above is suitable for this purpose, and will be employed.

Conversely, to characterize a detector, a calibrated broadband source with a known spectrum is necessary, such as a black body. Several types of well-characterized sources are available and can be employed to measure spectral responsivity of receiver devices. The spectral NEP (noise equivalent power) of a detector can be obtained if the noise spectrum of the source is known.

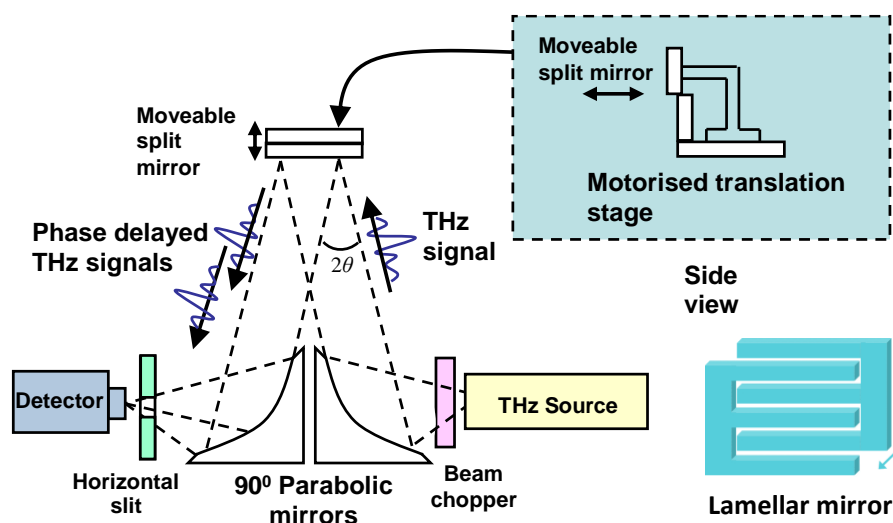
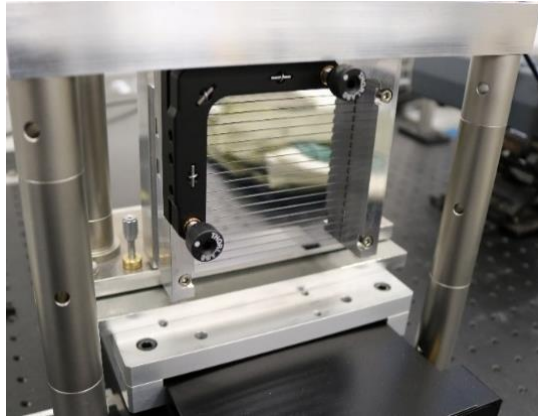


Figure 3. Schematic drawing of a lamellar interferometer and a split mirror.





**Figure 4. Photograph of the lamellar split mirror at NPL.**

The operational bandwidth of the interferometer is determined by the number ( $N$ ) and height ( $h$ ) of the lamellae. The ratio of maximum to minimum frequency is roughly equal to the number of lamellae in each half of the mirror:  $f_{\max}/f_{\min} \approx N$ . The maximum wavelength is set by the lamellae height:  $\lambda_{\max} < h/2$ . The parabolic mirrors used for input/output must have diameter at least as large as the total height of the lamellar mirror. To maximize optical throughput, the width of the lamellar mirror should be equal to or larger than its height.

The instrument designed and built at NPL has a mirror with 20 lamellae in each half, each with a height of 2.5 mm (shown in Figure 4), making a mirror with a total height & width of 105x105 mm. Its bandwidth at maximum sensitivity is therefore from 300 GHz to 6 THz. However, the shallow fall-off at lower frequencies allows measurements to be carried out down to <100 GHz.

The frequency resolution of a Michelson interferometer is determined by the scanning length of the moveable mirror, and is given by  $\Delta f = c/2L$ , where  $c$  is the speed of light in air and  $L$  is the scanning length (with the factor 2 arising due to double-pass). Typical achievable resolutions are of the order of 1 GHz, which is much coarser than that of a signal analyzer. Unlike electronic spectrum analyzers, a free-space lamellar interferometer is not a commercial instrument. Attention therefore must be given to its testing and calibration. The bandwidth, however, is very large: with a suitable detector, a bandwidth of a decade or more is easily obtainable. Moreover, because these devices operate in free-space, the bandwidth is not limited by waveguide transmission.

The SLT pyroelectric detector was used for the beam profile measurements. The frequency uncertainty in the peak position is determined by the data point spacing, which was at best 1 GHz.

### **2.1.3 Emitter beam profile**

Characterization of emitter (transmitter) beam profiles and detector (receiver) acceptance cones has long since been accepted as an essential tool in designing microwave and millimeter wave communication systems. There are extensively developed and well understood techniques for antenna characterization [4], and specialized facilities are available to perform the required measurements. None of these as yet exist for THz devices. Electronic THz emitters produce relatively low powers (commonly <100  $\mu$ W), have short wavelengths (<1 mm), and there is a lack of compact, high-sensitivity detectors. These factors combine to make spatial characterization of THz beams severely challenging.

There are currently several types of THz cameras on the market, with varying pixel numbers, spatial resolution, and frequency-dependent responsivity (e.g. [5, 6]). As tools for characterizing emitter beam profile, these present several challenges. First and foremost, it is necessary to account accurately for the spectral and spatial effects of the collecting and/or focusing optics, which are required because the sensor area of the camera is much smaller than the cross-section area of the THz beam to be examined. Furthermore, such cameras have a frequency-dependent responsivity, and do not perform as traceably calibrated power detectors. Finally, there may be issues related to cross-talk or spill-over between adjacent pixels.

The simplest technique for observing the beam profile of an emitter is to employ a detector with a small aperture, which is raster scanned across the beam area while recording the received power (Figure 5). This is repeated at different distances from the emitter to derive beam divergence. Alternatively, the detector may remain stationary, with the whole of the beam being collected and focused onto it (by mirrors or lenses), while only the aperture is scanned across the beam. In this case care must be exercised to avoid errors due to edge diffraction at the aperture. The spatial resolution is limited by the emitter power and detector sensitivity. This method will be the first-step approach adopted for emitter beam profile characterization. Good accuracy is easily achieved using this technique, and its implementation is straightforward, but it is slow and cumbersome. Since only power is measured, it also suffers from inability to provide phase information. However, there are currently no available alternative techniques offering better performance.

The SLT pyroelectric detector was used for the beam profile measurements. The amplitude uncertainty of each data point was approximately 10%. However, since this was random error, the resulting uncertainty in the beam profile was only around 5%. The position uncertainty was  $\pm 0.1$  mm.

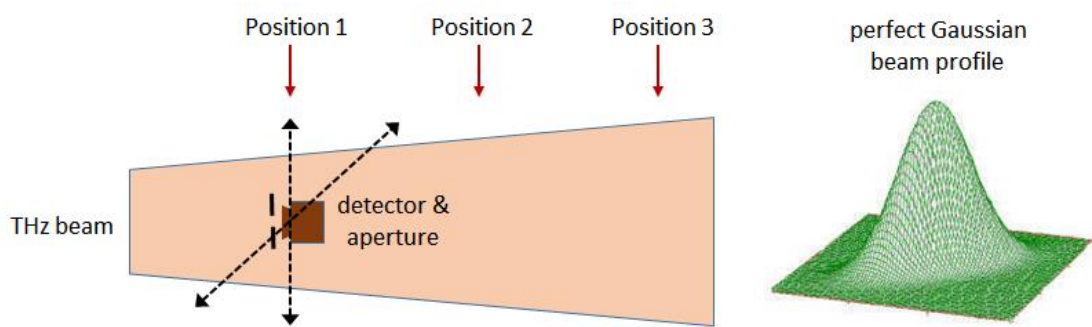


**Figure 5. Schematic drawing of beam imaging by aperture scanning.**

## 2.2 Results

### 2.2.1 Broadband frequency measurements

Frequency profile measurements were carried out on a commercial source, Topptica TeraScan continuous-wave frequency-tunable emitter, which is expected to be broadly similar in its behaviour to the emitters employed by TERAPOD. Figure 6 shows an example of lamellar interferometer output and the obtained frequency spectrum at 300 GHz (a.u. stands for arbitrary units). Frequencies between 100-600 GHz were measured. No higher harmonics or other spectral features were observed at any frequency. The results demonstrated satisfactory performance by the lamellar interferometer.

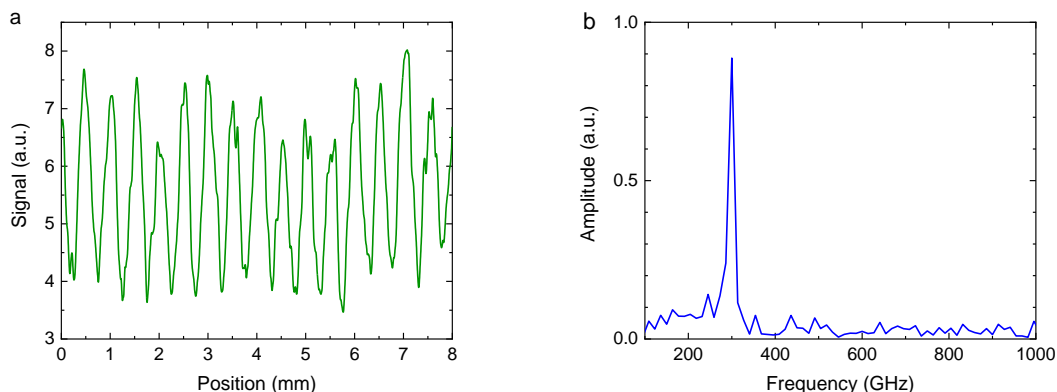


**Figure 6. Frequency measurements using lamellar interferometer and Topptica source at 300 GHz: a) interferometer signal; b) calculated spectrum.**

## 2.2.2 Beam profile measurements

Beam profile measurements were carried out on two commercial emitters: Toptica TeraScan continuous-wave frequency-tunable emitter, and Menlo Tera K15 pulsed broadband emitter. The Toptica emitter was set at different frequencies in order to observe the variation of the beam profile as a function of emitted frequency.

Figures 7 and 8 show examples of beam profiles from the Toptica and Menlo emitters respectively. It is seen that the continuous-wave narrow-line emitter (Toptica) has some distinct frequency-dependent features, whereas the pulsed broadband emitter (Menlo) has a nearly Gaussian profile. These results demonstrated satisfactory sensitivity and spatial resolution of the beam profiling setup.

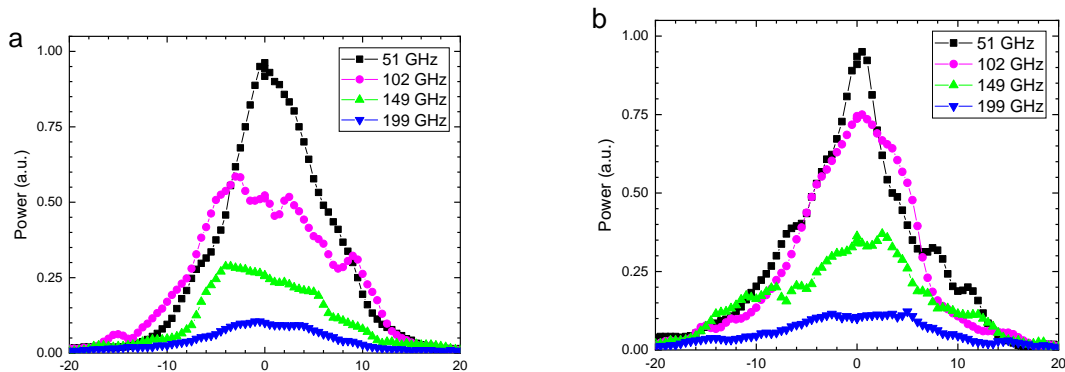


**Figure 7. Beam profiles from Toptica emitter at different frequencies, measured along the horizontal and vertical axes.**

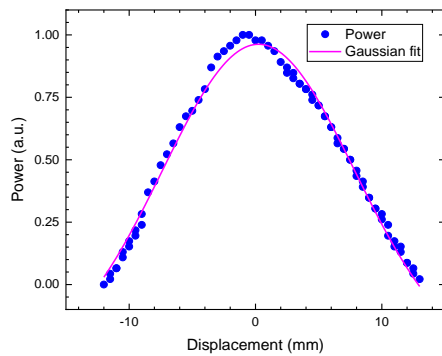


**Figure 8. Beam profile from Menlo emitter and a Gaussian fit (data from two axes overlap).**

### **3 Conclusion/Further work**

This report describes the equipment that was designed and built for characterising devices, specifically a lamellar interferometer for measuring broadband frequency spectrum, and a setup for determining the beam profile of emitters. Since no TERAPOD devices have been delivered to NPL by the project partners, the characterisation equipment was tested and validated by carrying out measurements on two commercial emitters. Both instruments demonstrated satisfactory performance. Further work on the equipment includes improving the SNR of the lamellar interferometer and automating the beam profile measurements. The most important aspect of future work is to carry out characterisation on devices provided by TERAPOD partners. A route to delivery of TERAPOD devices to NPL has been agreed by the project partners and a taskforce has been established in WP3 to ensure delivery.

## References

- [1] <http://www.pyrosensor.de/index-engl.html>
- [2] Müller R., Gutschwager B., Hollandt J., Kehrt M., Monte C., Müller R., Steiger A., “Characterization of a large-area pyroelectric detector from 300 GHz to 30 THz”, *J. Infrared Millimeter Terahertz Waves*, 36, 654-61 (2015).
- [3] M. Naftaly, P. Dean, R.E. Miles, J.R. Fletcher, A. Malcoci, “A Simple Interferometer for the Analysis of Terahertz Sources and Detectors”, *IEEE J Select Topics Quantum Electron* 14 (2008) 443-448.
- [4] C. A. Balanis, *Modern Antenna Handbook*, Pt IV, John Wiley & Sons, 2011.
- [5] <http://terasense.com/products/sub-thz-imaging-cameras/>
- [6] <https://www.ino.ca/en/products/terahertz-camera-microxcam-384i-thz/>